



EXPERIMENTAL INVESTIGATION OF SULPHIDE ION PERFORMANCE ON THE GROWTH OF CdZnS NANOPARTICLES

¹Ibiyemi, A. A., ¹Olubosede, O., ²Awodele, M. K., ²Akinrinola, O. and ²Awodugba, A. O.

¹Department of Physics, Federal University Oye Ekiti, Nigeria

²Department of Pure and Applied Physics, Ladoko Akintola University of Technology, Ogbomosho, Nigeria.

Corresponding authors email: abideen.ibiyemi@fuoye.edu.ng

ABSTRACT

It has been well established in this research work that sulphide ion play a crucial role in chalcogenide semiconductor devices. The impact of sulphide ion content (S^{2-}) on the surface morphology, optical, electrical and micro-structural properties of chemically deposited CdZnS nanoparticles was examined. The nanoparticles were prepared using cadmium sulphate as Cd^{2+} source, zinc sulphate as Zn^{2+} source and thiourea as S^{2-} source. NH_4OH was used as the complexing agent. The thiourea concentration was varied between 0.075 M – 0.580 M while the concentration of $ZnSO_4$, $CdSO_4$ and NH_4OH were fixed. EDX was used to confirm the compositional elements of the nanoparticles which are Cd^{2+} , Zn^{2+} , S^{2-} and little content of Si and O_2 . The SEM analysis revealed good uniformity and densely packed structure. Sulphide-rich nanoparticles exhibit large crystallite size compare to sulphide-poor nanoparticles. XRD indicates hexagonal structure (002) without phase transition. S^{2-} -rich CdZnS revealed less polycrystallinity compare to S^{2-} -poor CdZnS samples which exhibit better polycrystallinity. The crystallite size varied between 10 nm to 52 nm. The dislocation density increases from 0.000852 to 0.00242 $Line^2/m^2$ and then decreased to 0.000364 $Line^2/m^2$. Other microstructural properties such as lattice parameter and micro-strain as well as their relation with grain boundary surface area were also discussed. The best transmittance of about 97% was revealed. The layers deposited with high S^{2-} content showed less percentage transmittance and exhibit narrow energy band gap. The electrical resistivity is decreased while electrical conductivity increases with increasing S^{2-} content. The sheet resistance, charge carrier mobility and charge carrier density were also discussed.

Keywords: CdZnS, nanoparticles, transparent, lattice mismatch, SEM, grain boundary, band gap.

INTRODUCTION

Transparent conducting materials with high optical percentage transmittance are important elements for optoelectronic and display devices. A good transparent conducting layer must exhibit high optical energy band gap and high percentage transmittance. In addition, it shows much interest for blue and ultraviolet (UV) optical devices such as light-emitting diodes and laser diodes [1]. Wide band gap semiconductors are known to have a series of technological applications, such as transparent conducting electrodes, dye-sensitized solar cells and chemical sensors [2]. They are more attractive due to their luminescence characteristics [3-4]. Nanocomposites and Chalcogenide nanostructures have been extensively studied and have been one of the most important semiconductor nanomaterial research areas as a result of their valuable optoelectronic properties as well as photocatalytic properties. The chalcogenide nanostructure showed useful applications in photodegrading environmental pollutions [5]. Chalcogenide substance such as ZnS is one of the best semiconductors discovered and it has naturally shown remarkable versatility and effectiveness for novel properties and diverse applications. The nanoscale morphologies of ZnS was reported to be one of the

best among all inorganic semiconductors [6]. The morphology and size of ZnS nanoparticles were controlled by varying the amount of the sulfur content. The surface of ZnS was modified with tiny CdS nanoparticles through natural electrostatic attraction. The surface modification allows the formation of uniform ZnS–CdS nanocomposites. The nanocomposite of ZnS–CdS possess good photocatalytic performances. This is as a result of effective charge separation and increased specific surface area by the incorporation of CdS [5].

The thin films of ZnS powder fabricated on Si substrate by evaporation exhibit both hexagonal and cubic phase. The annealed of the film sample at temperature 700°C introduced a phase change. The cubic phase was transformed into the hexagonal ZnO phase. During the process of annealing, O_2 atoms from the atmosphere acquired sufficient energy thereby segregated Zn–S bond. The sulfur atoms are replaced by O_2 atoms in the lattice and sulfur atoms seem to diffuse into substrate and/or diffused out of the sample [7]. The average crystalline size of cubic phase of Ni: CdZnS nanoparticles and optical absorption measurements was smaller than that of cubic phase of CdZnS nanoparticles. The optical characteristics of Ni: CdZnS showed that the absorption edge of Ni: CdZnS

nanoparticles slightly shifts towards the lower wavelengths compare to undoped CdZnS nanoparticles. The Ni doping level in CdZnS altered the energy band gap. The energy band gap of CdZnS nanoparticles increases with Ni doping level in the CdZnS structure (3.75 eV to 4.02 eV) [8]. ZnS doped Cu exhibit densely and closely packed structure and formed compact morphology. The incorporation of Cu atoms into ZnS does not alter the particle size of the layers when the Cu doping level is low. The Cu doping level in ZnS influenced the structural formation of the particles in the sense that no X-ray diffraction peak was revealed at low Cu doping level (less than 5% Cu atoms) while diffraction peaks were revealed at high Cu doping level greater than 5%. This indicates that the Cu²⁺ ions are uniformly dispersed into the ZnS matrix and this is caused by low Cu atoms in the ZnS. Under controlled conditions, Cu²⁺ ions distribute homogeneously within the ZnS matrix by the virtue of substitution of Cu²⁺ ions for Zn²⁺ ions creating effective lattice defects due to their different electro-negativity. Since Cu is known to be an acceptor, the impurities create additional holes within the system and the Cu²⁺ level shifts down with increasing Cu concentration. Conclusively, the Fermi level moves away from mid-gap position toward the valence band edge [9].

It has been well established in this research work that CdZnS is useful as transparent electrode in solar cell and in various optoelectronic devices. For effective solar cell, solar energy spectrum entering the solar cell component is converted into useful current and this can be achieved by allowing the window layer of the solar cell device to be transparent to large spectrum of solar energy. The transparency of the window layer will reduce the optical losses in the solar cell and allow the production of useful amount of photogenerated current. This could only be achieved by lowering the optical losses. Only semiconductor material which exhibits high energy band gap and high percentage transmittance can be essentially used to achieve this [10]. The CdZnS films show recordable advantages for solar cell application due to some important qualities such as large energy band gap and high percentage transmittance of the material. The material exhibits wide energy band gap larger than 2.5 eV as compared to the CdS films [11]. The wide energy band gap of the layer caused low optical loss. This property makes it to be an effective replacement for CdS in semiconducting solar cell systems [12]. To the best of our knowledge, no report has ever been established on the study of variation of sulphide ionic content on the properties (electrical, optical, structural and surface morphology) of CdZnS nanoparticles. Attempts were then made in this research work to synthesis CdZnS nanoparticles with the intention of establishing potential usage of sulphide-poor and sulphide-rich based CdZnS devices. CdZnS is useful as a unique candidate for a wide energy band gap application. The energy band gap could be tuned by varying the constituent element such as Zn²⁺, Cd²⁺ and S²⁻ of the material [13]. In this research work, CdZnS is deposited by varying the S²⁻ content. This caused the formation of minimum lattice

mismatch and reduce the recombination velocity thereby produce better photogenerated current. Charge carrier mobility of semiconductor layers depends on the particle size. Large grain size traditionally lower the charge scattering center, low grain boundary surface area and low inter grain barrier height. All these affect the charge carrier mobility of semiconductor [14].

A number of film deposition methods such as spray pyrolysis, sputtering, electro deposition, vacuum evaporation, chemical vapour deposition and chemical bath deposition (CBD) have been

used for preparing II-VI compounds [15-18]. In this research work, CdZnS nanoparticles were prepared by doping CdZnS layer with various concentration of S²⁻ content using microwave assisted chemical bath deposition (MWCBD) technique.

METHODOLOGY

CdZnS samples were deposited on the glass substrates. The substrates were first cleaned with detergent (liquid) to remove any particles like dust which might interact with deposited layers. The substrates were later dipped in ethanol for the purpose of degreasing so as to remove particles such as grease, oil and metal oxide which cannot be removed using detergent and later rinse with deionize water and dried in air before deposition. The CdZnS nanoparticles were prepared by Microwave-assisted Chemical Bath Deposition (MWCBD) technique on commercial glass slide. The bath constituents were cadmium sulphate as source of Cd²⁺, ammonium hydroxide as complexing agent, Zinc sulphate as source of Zn²⁺ and thiourea as source of S²⁻. The solution bath comprises of 0.250 M cadmium sulphate, 0.580 M ammonium hydroxide and 0.375 M zinc sulphate. A 25 ml of each solution was taken into a separate beaker. Deionised water was added to fill up to 100 ml. NH₄OH was added drop-wise to the mixture to maintain a pH of 11. The pre-cleaned substrates were dipped into the chemical bath for a deposition time of 10 minutes. The depositions were carried out in a microwave oven at a temperature of 90°C and pH 11. 10 ml of NaOH was mixed with the solution in order to stabilize the pH. After the required time of deposition, the substrates were taken out from the solution bath, rinsed with de-ionized water to remove the loosely bonded molecules and subsequently desiccated in air.

The deposition is operated on the slow and/or controlled release of metal ions such as Zn²⁺ and Cd²⁺ and sulphide ions (S²⁻) in solution bath. During the process, the release of metal ions is controlled by complexing agent (NH₄OH). The deposition process started with nucleation and later followed by growth of the material. The released atoms were condensed and subsequently deposited on the substrate for proper growth. It is well known that the tendency of Zn²⁺ to form hydroxides is higher in magnitude than that of Cd²⁺ due to solubility products of Zn(OH)₂ which is 8.0 x 10⁻¹⁷ and Cd(OH)₂ which is 2.0 x 10⁻¹⁴. The solubility product of zinc is almost two orders of magnitude higher than Cadmium. But the tendency of sulphide

formation is lower for zinc ion. In spite of this, more zinc atoms were formed during the growth. During the deposition, the S^{2-} doping level determine the amount of sulphide ions that will be substituted for either Zn^{2+} or Cd^{2+} in the lattice. Highly transparent CdZnS nanoparticles were achieved by substitution of Zn^{2+} ions at S^{2-} sites in the lattice. Low sulphide-doping level is preferred because, at moderate doping levels, it tends to form segregated clusters with low particle size in the lattice. The surface morphology was characterized using Scanning Electron Microscopy (SEM). A Perkin-Elmer Lambda 900 spectrophotometer was used to obtain the optical parameters such as transmittance and absorbance. The electrical resistivity, electrical conductivity, charge carrier mobility and carrier concentration were evaluated by Hall Effect measurements at room temperature in a Van der Pauw four-point probe configuration, using indium contacts with a magnetic induction of 0.65 T.

RESULT AND DISCUSSION

CdZnS nanoparticles exhibit promising properties such as high percentage transmittance in the visible spectrum and low electrical resistivity which makes it a very important transparent conductor in a variety of optoelectronics devices such as solar cell. In this research work, CdZnS nanoparticles were deposited on pre-cleaned glass by varying the S^{2-} content in the solution bath. This was done by varying the thiourea concentration. The optical and electrical properties of the CdZnS layers were

investigated as a function of S^{2-} -doping level. The results showed that a transparent CdZnS layers were obtained with low S^{2-} content. An active transparent electrode made of CdZnS is obtained using low S^{2-} content. During the deposition, the solution mixture revealed yellow color (light yellow) and the solution mixture becomes deeper (deep yellow) as S^{2-} content is increased. This could be due to different rate of chemical reaction. Solution mixture of the deposition bath revealed deep yellow color using more sulphide ion content and this may be as a result of complete chemical reaction. The rate of formation of the nanocrystals is faster with high S^{2-} content in the solution bath. S^{2-} content determines the rate of deposition and the formation of nanocrystal. The rate of the reaction is faster using more thiourea concentration. At low thiourea concentration, transparent layers were formed and this is as a result of incomplete chemical reaction. Figure 1 depicts the EDX spectral showing the elemental composition of the deposited layers. The spectra revealed the presence of Zn^{2+} , Cd^{2+} and S^{2-} atoms and some other elements such as silicon, oxygen and carbon in the samples. The silicon peak shown may be due to diffusion of silicon atoms from amorphous glass substrates. The presence of oxygen is as a result of incomplete chemical reaction which indicates that all the oxygen from NH_4OH (complexing agent) were not completely oxidized. Complete oxidation of the chalcogenide metal was avoided in order to obtain nanoparticles with good transparency and better conductivity.

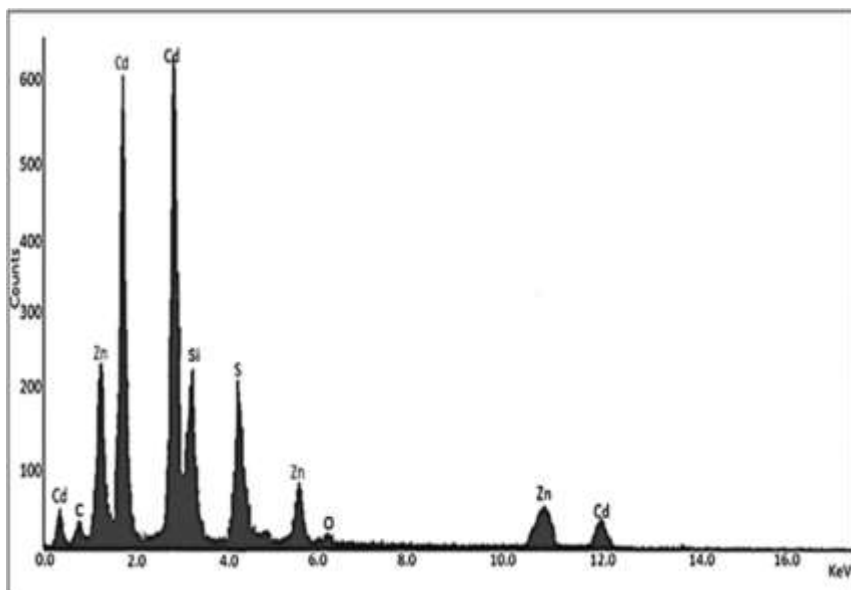


Fig. 1: Elemental composition of CdZnS nanoparticles.

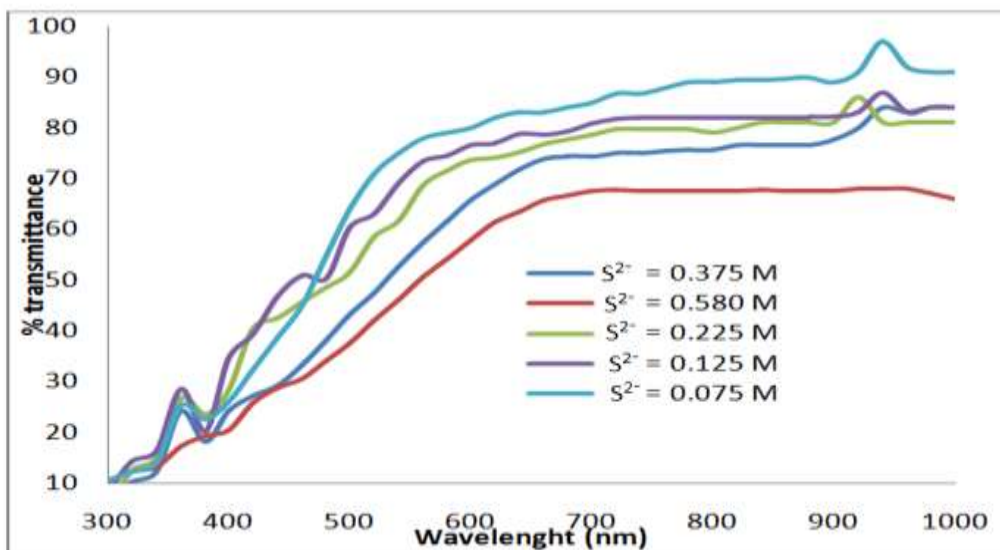


Fig. 2: Transmittance spectra of CdZn nanoparticles.

Figure 2 shows the percentage transmittance of CdZnS layers. The percentage transmittance is decreased as S^{2-} content is increased. The percentage transmittance 97% and 57% were revealed with 0.075 M and 0.580 M of S^{2-} content. Lowest transmittance was obtained with 0.580 M of S^{2-} . This implies that high S^{2-} content is not well suitable to be useful as transparent electrode of solar cell due to reduced percentage transmittance. This is probably attributed to an increase of the carrier concentration. A good transparent layer was obtained using low sulphide ion concentration. The nanoparticles deposited with low S^{2-} content is a good compound for efficient window layer of solar cell due to its better transparency within visible region. It allows much photon to be trapped by absorber layer and convert it to usable voltage.

The crystal structure and microstructural properties of CdZnS nanoparticles deposited were examined using X-ray diffraction (XRD) technique. The X-ray diffraction patterns of CdZnS nanoparticles are depicted in figure 3. The structural analysis clearly explains the impact of S^{2-} on the crystallinity of the deposited layers. The X-ray diffraction revealed diffraction peaks associated with (101), (112), (100), (103) (110), (102), and (002) planes. All the deposited layers of CdZnS revealed (002) direction as the preferential orientation. Other diffraction peaks such as (101), (200), (110) and (102) disappeared with increasing S^{2-} content. Only (100), (112) and (002) were not disappeared. The layers exhibit hexagonal phase. The nanoparticles are polycrystalline in nature and the

polycrystallinity is reduced as S^{2-} content is increased. The presence of many peaks indicates the polycrystalline structure of the nanoparticles. The incorporation of S^{2-} leads to reduction of the intensity of diffraction peaks of (002) preferred orientation. This could be as a result of dormant S^{2-} atoms in the CdZnS nanoparticle which is unable to segregated into grain boundaries and not able to affect the crystallization of the preferred orientation. It is noted that the polycrystallinity of CdZnS nanoparticles decreases with increasing S^{2-} doping level. This could probably be the reason for disappearing of XRD peak intensity. The polycrystallinity of CdZnS deposited is decreased with increasing S^{2-} content as a result of excess sulphide atoms which do not occupy the proper lattice positions but occupying interstitial sites. The crystallites present in a polycrystalline material naturally possess a crystallographic orientation which could be different from that of its neighbors. The orientation of the crystallites which is referred to as the preferential orientation may be distributed randomly with respect to selected frame of reference. The preferential orientation factor $f(hkl)$ of the crystalline plane with respect to other observed peaks from the plane is evaluated by calculating the fraction of the peak intensity of that particular plane over the sum of the intensities of other peaks. The values of the preferential orientation factor $f(hkl)$ of the intensity peaks is shown in table 1. (002) plane exhibits better preferential orientation factor which is an indication that there is a strong orientational growth along the (002) plane.

Table 1: Preferential orientation factor of CdZnS nanoparticles at different S²⁻ doping content.

S ²⁻ doping content	f(100)	f(002)	f(101)	f(102)	f(110)	f(103)	f(112)
0.075	0.2234	0.2608	0.1274	0.1500	0.1501	0.1616	0.1170
0.125	0.2207	0.3529	-	0.1898	-	0.1819	0.2876
0.225	0.3720	0.4615	-	-	-	0.2321	0.1896
0.375	0.6551	0.7408	-	-	-	-	0.2307

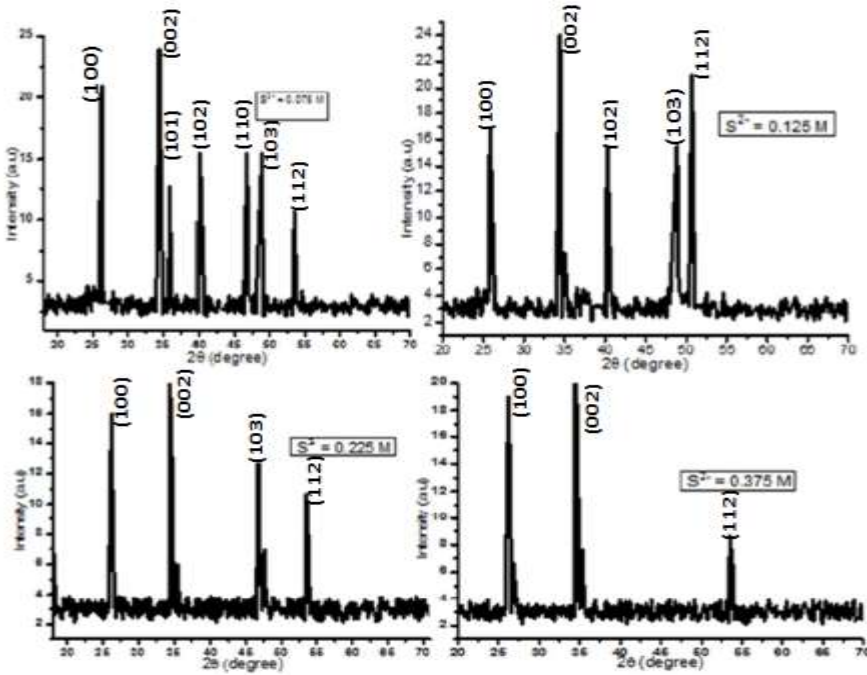


Fig. 3: XRD spectra of CdZnS nanoparticles.

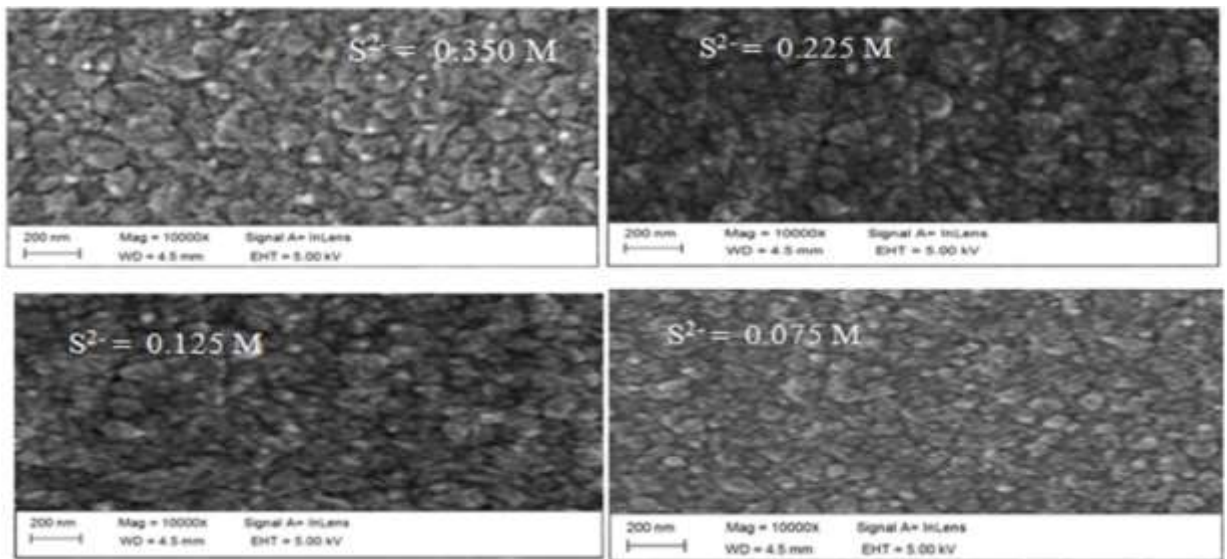


Fig. 4: SEM micrograph of Cd_{1-x}Zn_xS nanoparticles.

SEM images of CdZnS nanoparticles are shown in figure 4. The deposited layers are homogeneous showing well grown grains and smooth surface. These surface properties revealed better crystallinity which is a good device characteristic. It is clear from these micrographs that the surface morphology of CdZnS samples are modified by S^{2-} doping level. CdZnS nanoparticles showed uniform surface without any hole, rupture or fractures and the substrates are well covered by the deposits. The surface

morphology shows the clusters composed of particles of distinct sizes. Hence, the average cluster size was determined from distinct clusters of the nanoparticles in the range 60 – 100 nm. The decrease in sulphide ion content revealed an improvement of the clusters size diameters within 80-120 nm. This may be due to agglomeration of smaller nanoclusters forming larger clusters^[19]. The grain size gradually increased with S^{2-} doping level.

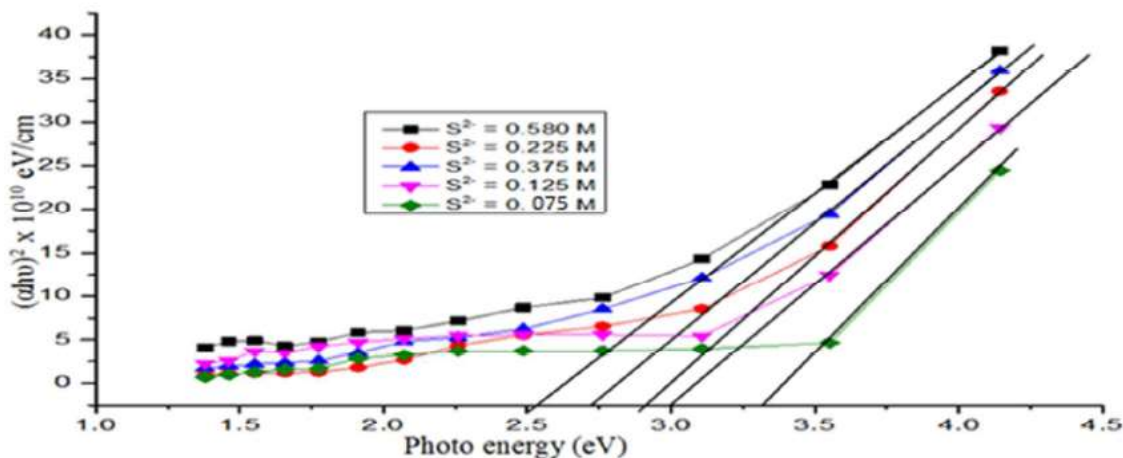


Fig. 5: Energy band gap of CdZnS nanoparticles.

The energy band gap (E_g) of the CdZnS nanoparticles is depicted in figure 5. The E_g of the nanoparticles was estimated as a function of photon energy ($h\nu$) and determined by experimentally observed the values of $(\alpha h\nu)^2$ against $(h\nu)$. The energy band gap varied between 2.52 - 3.40 eV. The optical band gap of the deposited layers is reduced with increasing S^{2-} doping level. The S^{2-} tuned the energy band gap of the deposited layers because at different sulphide ion content, the energy gap does not remain the same. A good optical band gap 3.40 eV was revealed with 0.075 M of S^{2-} . High S^{2-} concentration yielded low energy band gap. It was noted that S^{2-} causes the energy band gap of CdZnS layers to be tunable depending on its concentration in the solution bath. Thus, a sulphide-poor CdZnS showed wide energy band gap which can be recommended for optoelectronic device application.

A wide energy band gap indicates an increase in transmittance. This is in agreement with the transmittance results. The decrease in energy band gap as the S^{2-} concentration can be attributed to the less formation of the CdZnS nanocrystals. In this research work, we emphasized the transmittance data because the change in the optical response induced by the presence of the sulphide atoms is several times larger at low S^{2-} content. The transmission

results are, however, fully consistent with the energy band gap measurements and it is in agreement with the literature.

Using low S^{2-} content, bands are formed as a result of the merging of adjacent energy levels of a low number of atoms due to low crystallite size. Therefore, the number of overlapping orbitals or energy level is decreased and the width of the band gets narrower. This causes an increase in energy gap between the valence band and conduction band and responsible for wide energy gap in CdZnS with low S^{2-} content. At high S^{2-} content, the size of the particles is large and this is produced due to agglomeration of much number of atoms. In this regard, the number of overlapping orbitals or energy levels and the width of the band is increased, therefore causes increase in the energy band between the valence band and conduction band. As a result of this, the optical energy band gap is narrowed. In the UV region, all the deposited layers exhibit low percentage transmittance showing that the materials are less transparent to UV. This quality assists CdZnS to be useful in architectural window coatings. The high absorbance in the UV region makes the material to be a good absorber of UV radiation. As a result of this, UV radiation is screened off and the infrared and visible radiation is admitted into the building.

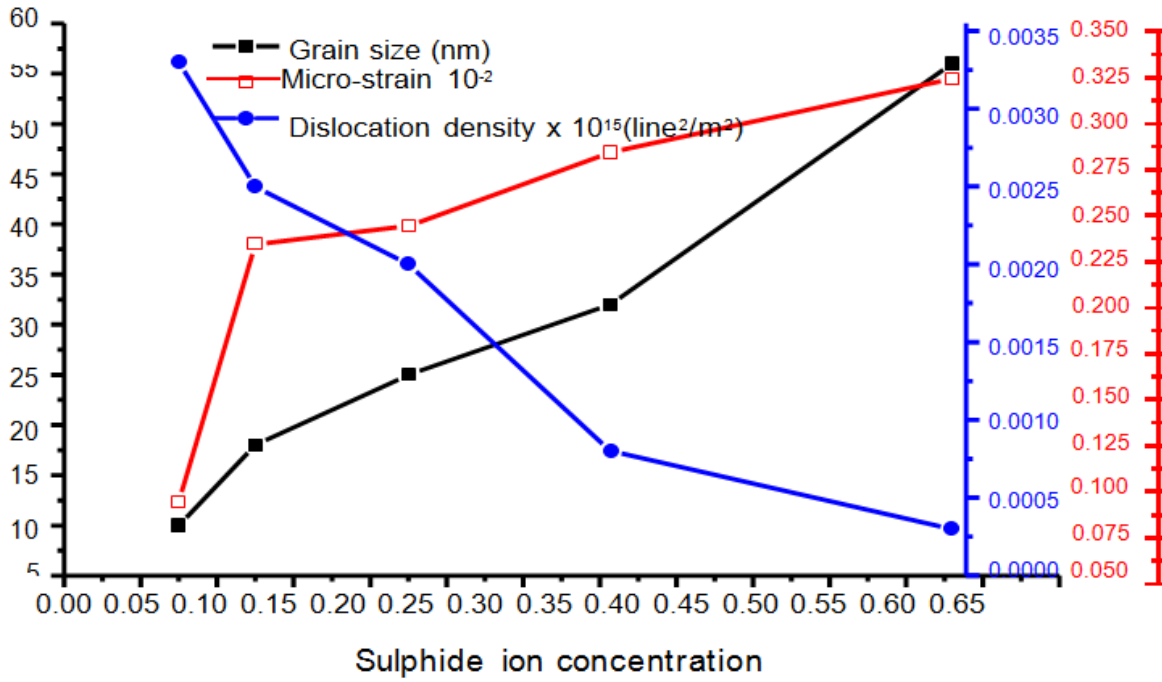


Fig. 6: Crystallite size, dislocation density and micro strain of CdZnS nanoparticles.

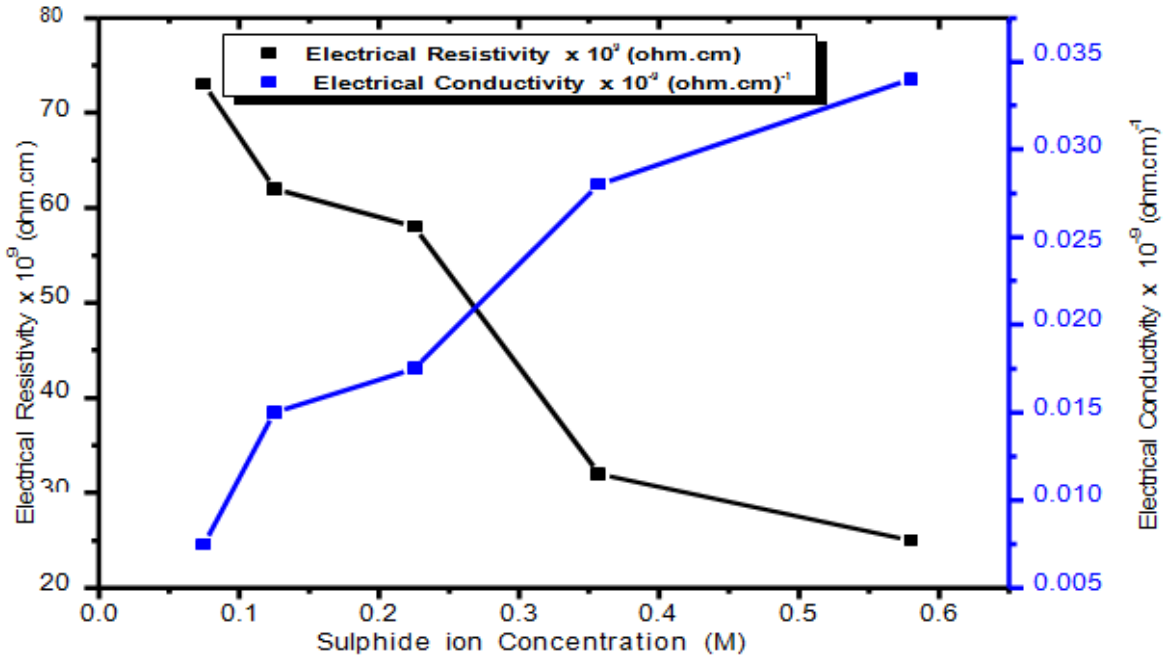


Fig. 7: Electrical conductivity and electrical resistivity of CdZnS nanoparticles.

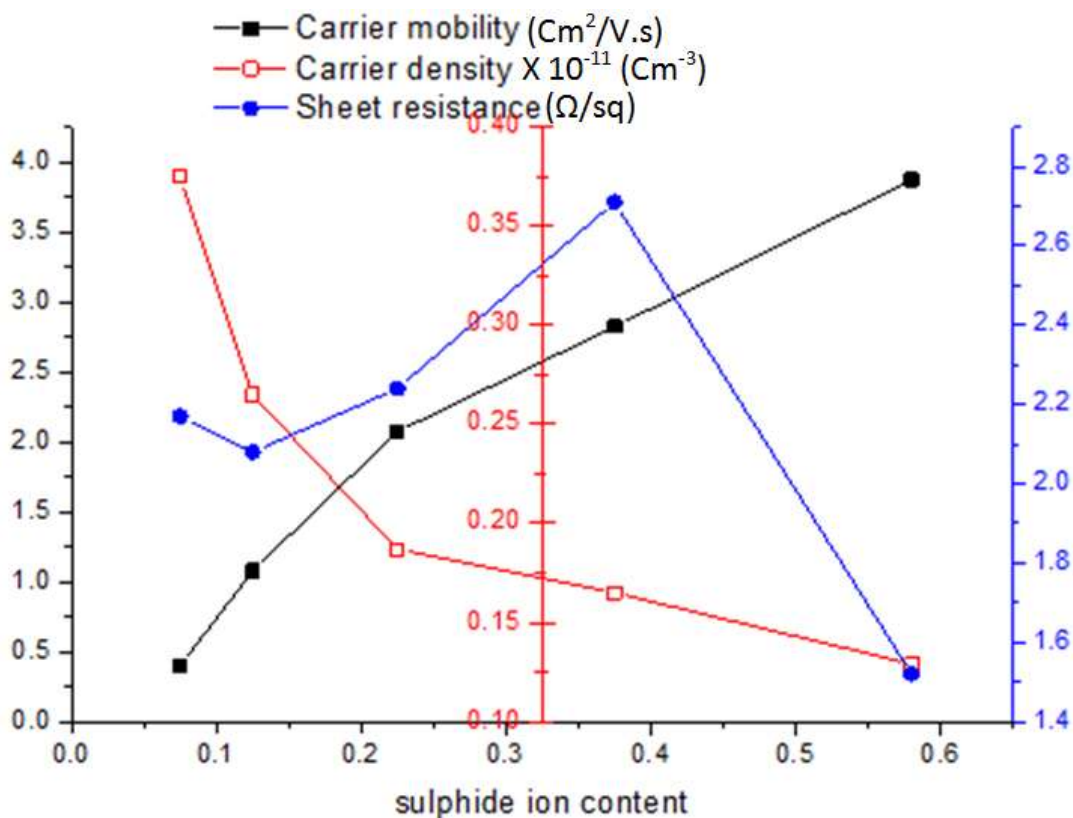


Fig. 8: Carrier mobility, carrier concentration and sheet resistance of CdZnS nanoparticles.

Figure 8 revealed the charge carrier mobility, charge carrier concentration and sheet resistance of CdZnS nanoparticles. The electrical properties of the deposited layers were tuned by varying the S²⁻ content in solution bath. The sheet resistance initially decreases from 2.24 Ω/sq (S²⁻= 0.075 M) to 2.07 Ω/sq (S²⁻= 0.125 M) and then increases 2.72 Ω/sq (S²⁻= 0.375 M) which was later decreases to 1.53 Ω/sq (S²⁻= 0.580 M). The charge carrier mobility increases and the charge carrier concentration decreases with increasing S²⁻ content. The electrical resistivity of the CdZnS nanoparticles deposited with low S²⁻ content is dominated by free carrier concentration. The charge carrier mobility is increased with increasing S²⁻ content which might possibly responsible for increase of the electrical conductivity. This increase could be attributed to crystallite size effect. The size of the grain of the nanoparticles increases with

increasing S²⁻ content. The large crystallite size formed low grain boundary surface area and produced better charge carrier mobility. The increase of the charge carrier mobility with increasing S²⁻ content in CdZnS could be attributed to decrease of stacking fault density as well as better grains orientation. This causes a decrease in the inter-grain barrier height due to large grain size. The increase of S²⁻ content in CdZnS enhances better lattice formation and this causes the decrease of grain boundary scattering centers due to increase in grain size. Therefore, the carrier mobility and electrical conductivity were better. The electrical resistivity of the CdZnS layers is decreased with increasing S²⁻ content. This could be attributed to size and dimension of the confinement. The lowest resistivity obtained with high sulphide ion content is well suitable for solar cells application.

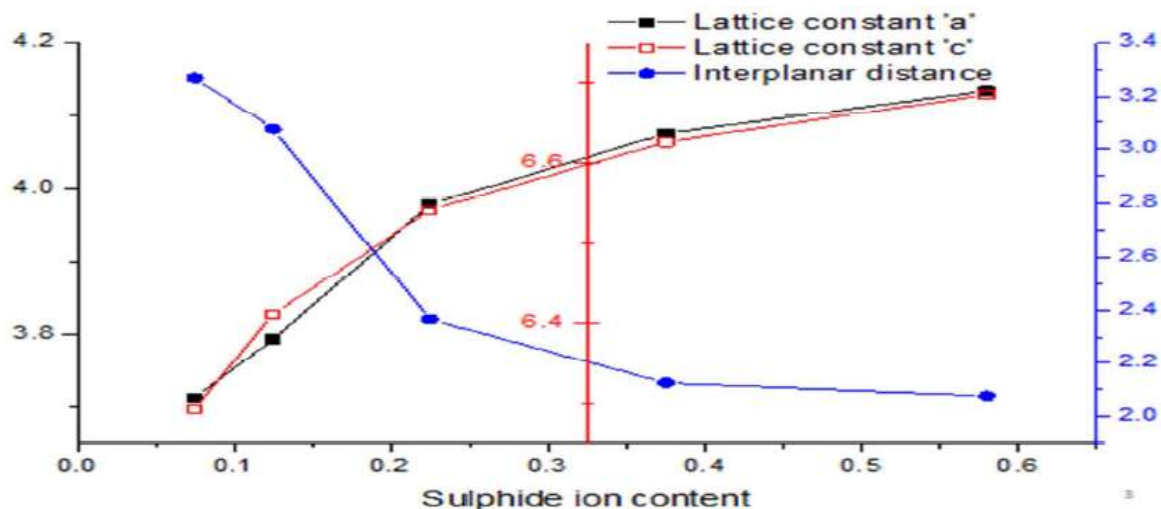


Fig. 9: Lattice constants and interplanar distance of CdZnS nanoparticles.

Figure 9 illustrate the lattice parameters and the interplanar distance of CdZnS nanoparticles. The lattice parameter increases with increasing S^{2-} content and this may be due to the incorporation of more S^{2-} nanocrystals in the lattice. In order to reduce the lattice mismatch between heterojunction partners, the lattice parameter must be same or having closer values. The material practically used as p-type absorber layer of solar cell are $CuIn_{1-x}Ga_xS_2$ (CIGS) with lattice parameter $\sim 5.5 \text{ \AA}$ and $CuIn_{1-x}Ga_xSe_2$ with lattice parameter $\sim 5.8 \text{ \AA}$ [20]. Therefore, a minimum lattice mismatch could be obtained with low S^{2-} content due to reduced value of the lattice parameter which is closer to 5.8 \AA . Using high S^{2-} content, the value of the lattice parameter of CdZnS is relatively high and not actually closer to lattice parameter of the CIGS. This introduced much lattice mismatch. Low lattice mismatch is required for better photovoltaic solar cell device performance. As S^{2-} content increases, lattice mismatch tends to be increasing due to increase in lattice parameter of deposited layers. The lattice parameters need to be closer in order to reduce the lattice mismatch and interfacial recombination velocity. The recombination process is responsible for the decrease in the number electron that contributes to amount of electric current that will be generated. In addition, high lattice mismatch causes more recombination velocity and therefore reduce the amount of current produced. The grain size of CdZnS nanoparticles increases with sulphide ion content as shown in figure 7. This is produced due to agglomeration of small nanoparticles and attributed to low grain boundary surface area which favors good electrical conductivity. As the sulphide ion content increases, the dislocation density decreases. High S^{2-} content is responsible for better structural formation which is good for electrical application. This property helps in avoiding the process that affect the electronic state or delay the electron transition.

CONCLUSION

Polycrystalline, transparent and n-type conductivity CdZnS nanoparticles were prepared on glass substrates using different sulphide ion concentrations. The CdZnS deposited layer is a good transparent electrode for solar cell application due to high percentage transmittance and low electrical resistivity. These qualities were revealed with low S^{2-} content. The effect of S^{2-} doping level on the structural, surface morphology, optical and electrical properties of the deposited layers was examined. XRD analysis confirmed the formation of hexagonal structure without phase change. The grain size of the films is increased with increasing S^{2-} content. The elemental composition of the deposited layers are Cd^{2+} , Zn^{2+} , S^{2-} and little content of Si and O_2 . The electrical resistivity of CdZnS increases with increasing S^{2-} . The optical energy band gap of the samples is decreased from 3.40-2.52 eV with increasing S^{2-} content. The electrical properties measured showed that the increase in electrical conductivity of CdZnS with increasing S^{2-} concentration is due to the increase of the grain size. Nanoparticles deposited with large grain size exhibit lower grain boundary surface area, lower inter-grain barrier height and minimum charge scattering center which affect the mobility of the charge carrier and the electric current generated. The nanoparticles deposited with low grain size exhibit low charge carrier mobility due to many scattering centers, large grain boundary surface area and inter-grain barrier height.

REFERENCES

- [1] El-Etre A Y and Reda S M. Characterization of nanocrystalline SnO_2 thin film fabricated by electro deposition method for dye sensitized solar cell application. Applied Surface Science, 2010, 256: 6601

- [2] Vilaseca M, Coronas J and Cirera A. Development and application of micro machined Pd/SnO₂ gas sensors with zeolite coatings. *Sensors and Actuators B: Chem*, 2008, 133: 435
- [3] Fang C, Wang S and Wang Q. Coralloid SnO₂ with hierarchical structure and their application as recoverable gas sensors for the detection of benzaldehyde/acetone. *Mater Chem Phys*, 2010, 122: 30
- [4] Kim T W, Lee D U, Yoon Y S. Microstructural, electrical and optical properties of SnO₂ nanocrystalline thin films grown on InP (100) substrates for applications as gas sensor devices. *Journal of Applied Physics*, 2000, 88: 3759
- [5] Xiaojie Xu, Linfeng Hu, Nan Gao, Shaoxiong Liu, Swelm Wageh, Ahmed A. Al-Ghamdi, Ahmed Alshahrie and Xiaosheng Fang. Controlled Growth from ZnS Nanoparticles to ZnS–CdS Nanoparticle Hybrids with Enhanced Photoactivity. *Advanced Functional Material*, 2014, 25:445-454
- [6] Xiaosheng Fang, TianyouZhai, Ujjal K Gautam, Liang Li, LiminWu, Yoshio Bando and Dmitri Golberg. ZnS nanostructures: From synthesis to applications. *Progress in Material Science*, 2011, 56 (2):175-287.
- [7] Mahmood.K, Asghar.M, Amin.N, and Adnan Ali. Phase transformation from cubic ZnS to hexagonal ZnO by thermal annealing. *Journal of Semiconductor*, 2015, 36 (3):0330011-0330012
- [8] Sabit Horoz, Mustafa Akyol, Ahmet Ekicibil and Ömer Sahin. Structural, optical and magnetic properties of CdZnS and Ni:CdZnS nanoparticles. *Journal of Materials Science: Materials in Electronics*, 2017, 28 (23):18193–1819
- [9] Mehrabian M., Esteki Z, Shokrvash H, and Kavei G. Optical and electrical properties of copper-incorporated ZnS films applicable as solar cell absorbers. *Journal of Semiconductor*, 2016. 37(10):1030021- 1030026.
- [10] Mahdi M.A. Band Gap Shift of Chemical Bath Deposition Cd_{1-x}Zn_xS Thin Films. *Journal of Basrah Researches (Sciences)*. 2009, 35 (6):70-75.
- [11] Zhou.J, Wu.X, Teeter.G, To.B, Dhere R.G and Gessert T.A. CBD Deposited Cd_xZn_{1-x}S Thin Films and Their Application in CdTe Solar Cell, *Phy. Stat. Sol*, 2004, 24 (13):775-778.
- [12] Ragesh. chandran, G. Suresh, A comparative study of physical and optical properties of CdZnS and CdNiS nanocrystalline films deposited by Chemical Bath Method, *Chalcogenide Letters*, 2011, 8(11):689-694.
- [13] Awodugba A.O, Ibiyemi A.A and Ajayi J.O. Effect of grain size on the electrical transport mechanism for zinc doped CdS thin films. *International Journal of Scientific Research and Management Studies*. 2014, 1(7): 234-241
- [14] Abideen A. Ibiyemi, Ayodeji O Awodugba, Olusola Akinrinola, and Abass A Faremi. Zinc doped CdS nanoparticles synthesized by microwave-assisted deposition. *Journal of Semiconductor*, 2017, 38 (9):0930021-0930026.
- [15] Dona.J.M., and Herrero.J. Chemical Bath Codeposited CdS-ZnS Characterization, *Thin Solid Films*, 2002, 268:5-12.
- [16] Illican S., Caglar Y and Caglar M. Effect of the Substrate Temperatures on the Optical Properties of the Cd_{0.22}Zn_{0.78}S Thin Films by Spray Pyrolysis Method. *Physica Macedonica*. 2006, 56:43-48.
- [17] Dzhabarov, T.D. Ongul, F., and Karabay, I. Formation of CdZnS thin films by Zn diffusion. *Journal of Applied Physics*. 2006, 39, 32-41.
- [18] Ravangave L.S and Biradar U.V. Study of Structural, Morphological and Electrical Properties of Cd_xZn_{1-x}S Thin Films. *IOSR Journal of Applied Physics*. 2013, 3 (3):41-47.
- [19] Al-Ani S.K., and Mahdi, M.A. Optical characterization of chemical bath deposition Cd_{1-x}Zn_xS thin Films. *International Journal of Nanoelectronics and Materials*. 2012, 5:11-24.
- [20] Akinrinola O., Ibiyemi A.A., Awodugba A.O and Faremi A.A. Numerical simulation of CZTS/ZnO/FTO hetero-junction solar cell. *FUOYE journal of Pure and Applied Science*, 2018, 2:21-27.